APOE4 disrupts intracellular lipid homeostasis in human iPSC-derived glia

As Published: 10.1126/scitranslmed.aaz4564

Publisher: American Association for the Advancement of Science (AAAS)

Persistent URL: https://hdl.handle.net/1721.1/136168

Version: Author's final manuscript: final author's manuscript post peer review, without publisher's formatting or copy editing

HHS Public Access

Author manuscript

Sci Transl Med. Author manuscript; available in PMC 2021 September 03.

Published in final edited form as:

Sci Transl Med. 2021 March 03; 13(583): . doi:10.1126/scitranslmed.aaz4564.

APOE4 disrupts intracellular lipid homeostasis in human iPSC-derived glia

Grzegorz Sienski[#1,12], **Priyanka Narayan**[#1,2,3], **Julia Maeve Bonner**[#1,2], **Nora Kory**[1], **Sebastian Boland**[4], **Aleksandra A. Arczewska**[5,12], **William T. Ralvenius**[2], **Leyla Akay**[2], **Elana Lockshin**[2], **Liang He**[6], **Blerta Milo**[2], **Agnese Graziosi**[2], **Valeriya Baru**[1,13], **Caroline A. Lewis**[1], **Manolis Kellis**[9,10], **David M. Sabatini**[1,7,8,9,11], **Li-Huei Tsai**[2,9,*], **Susan Lindquist**[1,7,8,†]

[1]Whitehead Institute for Biomedical Research, Cambridge, MA 02142, USA

[2]Picower Institute for Learning and Memory, Department of Brain and Cognitive Sciences, MIT, Cambridge, MA 02139, USA

[3]Genetics and Biochemistry Branch, NIDDK, National Institutes of Health, Bethesda, MD 20814, USA

[4]Department of Molecular Metabolism, Harvard T.H. Chan School of Public Health, Boston, MA 02115, USA

[5]Department of Stem Cell and Regenerative Biology, Harvard University, Cambridge, MA 02138, USA

[6]Duke University, Durham, NC, 27708, USA

[7]Massachusetts Institute of Technology, Cambridge, MA 02142, USA

[8]Howard Hughes Medical Institute, Cambridge, MA 02139, USA

[9]Broad Institute of Harvard and Massachusetts Institute of Technology, Cambridge MA 02142, USA

[10]Computer Science and Artificial Intelligence Laboratory, Massachusetts Institute of Technology, Cambridge, MA, 02139, USA

[11]Koch Institute for Integrative Cancer Research and Massachusetts Institute of Technology, Department of Biology, Cambridge, MA 02139, USA

[*]correspondence to lhtsai@mit.edu.

[†]deceased

Author contributions: GS, PN, L-HT, SL conceptualized the study. GS performed yeast screens, yeast genetics, and choline rescue experiments. Investigation (astrocytes, microglia, media analysis): GS, PN, JMB. Investigation: WR, SB, NK, AAA, LA, EL, LH, BM, AG, VB, CAL. Writing (original draft): GS. Writing (review and editing): GS, PN, JMB, MK, DMS, L-HT Supervision: MK, DMS, L-HT and SL. Funding Acquisition: GS, PN, DMS, L-HT and SL.

Competing interests: SL was a co-founder of Yumanity Therapeutics. LHT is a member of the Scientific Advisory Board of Yumanity Therapeutics. PN and SL are co-inventors on US Patent PCT/US2015/049674 (Cells expressing Apolipoprotein E and uses thereof). GS, PN, JMB, LHT are co-inventors on patent application 63/023,698 (Use of choline supplementation as therapy for APOE4-related disorders). GS and AAA are currently employees and shareholders of AstraZeneca. CAL is a paid consultant for ReviveMed Inc.

Data and materials availability: Plasmids used in the study have been deposited at Addgene with accession number #78653.

[12]Present address: Discovery Biology, Discovery Sciences, BioPharmaceuticals R&D, AstraZeneca, Gothenburg, Sweden

[13]Present address: Q-State Biosciences, Cambridge, MA 02139

[#] These authors contributed equally to this work.

Abstract

The *E4* allele of the apolipoprotein E gene (*APOE*) has been firmly established as a genetic risk factor for many diseases including cardiovascular diseases and Alzheimer's disease (AD), yet its mechanism of action remains poorly understood. APOE is known to function as a lipid transport protein, and the dysregulation of lipids has recently emerged as a key feature of several neurodegenerative diseases including AD. However, it is unclear how APOE4 perturbs the intracellular lipid state. Here, we report that *APOE4* disrupted the cellular lipidome in human iPSC-derived astrocytes generated from fibroblasts obtained from *APOE4* compared to *APOE3* carriers, and in yeast expressing human *APOE4* isoforms. We combined lipidomics and unbiased genome-wide screens in yeast with functional and genetic characterization to demonstrate that APOE4 induced widespread changes in lipid homeostasis. These changes resulted in increased unsaturation of fatty acids and an accumulation of intracellular lipid droplets in both yeast and human iPSC-derived astrocytes. Additionally, we identified genetic and chemical modulators of this lipid disruption. In particular, we show that a simple environmental change in the culture medium—supplementation with choline, a soluble phospholipid precursor—was sufficient to restore the cellular lipidome to its basal state in *APOE4* expressing astrocytes and in yeast expressing human APOE4. Our study illuminates key molecular disruptions in lipid metabolism that may contribute to the disease risk linked to the *APOE4* genotype. Importantly, our study suggests that manipulating lipid metabolism could be a therapeutic approach to help to alleviate the consequences of carrying the *APOE4* allele.

One Sentence Summary:

APOE4 disrupts intracellular lipid homeostasis in human and yeast cellular models, which was reversed by promoting phospholipid synthesis via choline supplementation.

Accessible Summary:

APOE4 is a strong genetic risk factor for many diseases, most notably, late-onset Alzheimer's disease. Sienski, Narayan, & Bonner et al., show that human glia with an *APOE4* genotype accumulate unsaturated triglycerides leading to a lipid imbalance. Using genetic screens in yeast, the authors discovered that choline supplementation, by promoting phospholipid synthesis, restores a healthy cellular lipid state in *APOE4* cells. The authors then demonstrate that choline supplementation can also restore lipid homeostasis in human *APOE4* astrocytes. These findings suggest that rewiring of the metabolic state of glia may reduce *APOE4*¬-associated disease risk.

Introduction

Genome-wide association studies implicate lipid metabolism in a number of late onset neurodegenerative diseases, including Alzheimer's Disease (AD) (1–5). The accumulation

of lipid (adipose saccules) in glia is a pathologically defining feature of AD (6). The most highly validated genetic risk factor for late-onset AD is the ε4 allele of the *APOE* gene (*APOE4*). *APOE* encodes a lipid-carrier protein that is a key component of many lipoprotein particles (7–9).

The human gene encoding *APOE* is polymorphic with three common coding variants (isoforms) differing from one another by two amino acids: ε3 (*APOE3*), ε4 (*APOE4*) and ε2 (*APOE2*) (10). The *APOE4* genotype is the primary genetic risk factor for late-onset AD (11–13), is associated with cardiovascular diseases (14, 15), increases risk for metabolic syndrome (16), and is linked with decreased lifespan (17). The presence of *APOE4* lowers the age of AD onset and increases the lifetime risk for developing the disease in a gene dose-dependent manner (18).

Apolipoprotein E (APOE) is a component of many lipoprotein particles and serves as a ligand for membrane receptors that mediate lipoprotein uptake (7–9). APOE4 has been suggested to contribute to AD pathogenesis by modulating multiple pathways including lipid transport and metabolism (19), however, the ways in which APOE4 alters the lipidome of cells remain unknown. In this study, we characterized the lipidome of *APOE4*-expressing human astrocytes generated from induced pluripotent stem cells (iPSCs) derived from fibroblasts from both *APOE4* and *APOE3* carriers (20). We found that iPSC-derived *APOE4* astrocytes in vitro accumulated unsaturated triacylglycerides stored in lipid droplets to a greater extent than did their isogenic *APOE3* counterparts. Using the conservation of lipid metabolism pathways between yeast and human cells (21–24), we established establish a yeast model where the expression of human *APOE4,* but not human *APOE3,* by yeast induced the accumulation of lipid droplets and increased unsaturation of triacylglycerides in a similar manner to iPSC-derived *APOE4* astrocytes. Lipid droplet accumulation was accompanied by a specific growth defect in *APOE4*-expressing yeast. Loss-of-function genetic screens revealed that perturbations in a lipogenic transcriptional program uncoupled *APOE4* from its cytotoxic effects. Promoting synthesis of the membrane lipid phosphatidylcholine by supplementing cell cultures with choline reversed the abnormal lipid unsaturation and lipid droplet accumulation in both the *APOE4* expressing yeast model and in human iPSC-derived *APOE4* astrocytes.

Results

Human iPSC-derived APOE4-expressing astrocytes display intracellular lipid dysregulation

We first characterized the impact of the *APOE4* allele on the lipidome of human iPSC-derived astrocytes. In the brain, astrocytes are the major source of APOE (25), and have previously been reported to show *APOE4*-specific defects (26, 27). We utilized two independent pairs of previously published isogenic iPSC lines, derived from either a parental *APOE3* or *APOE4* homozygote, that had been edited with CRISPR-Cas9 to make the corresponding *APOE3* or *APOE4* isogenic line. These lines were differentiated into astrocytes that expressed the astrocyte proteins GFAP and S100β (Fig. 1A, B) (27).

We compared the lipid composition of the *APOE3* and *APOE4* expressing human iPSC-derived astrocytes by performing whole cell lipidomic analysis using liquid chromatography-mass spectrometry (LC-MS) (28, 29). We observed a minor change in phospholipid content and a much larger increase in triacylglycerides in *APOE4*-expressing human iPSC-derived astrocytes compared to *APOE3*-expressing human iPSC-derived astrocytes (Fig. 1C). We also observed that the degree of unsaturation of the fatty acids attached to triacylglycerides in *APOE4* astrocytes was far higher than that in *APOE3* astrocytes (Fig. 1D). Triacylglycerides, along with other neutral lipids such as cholesterol esters are stored in cytoplasmic organelles called lipid droplets (30). We therefore stained our isogenic astrocytes using a lipophilic dye, LipidTox, that labels neutral lipids (31). After 2 weeks in culture, we observed that *APOE4* astrocytes accumulated a greater number of lipid droplets than did their *APOE3* counterparts (Fig. 1E), which was accompanied by accumulation of a lipid droplet-resident protein, Perilipin-2 (Fig. 1F) (32). We validated these findings in an additional pair of isogenic iPSC lines (Fig. S1A), again observing increased accumulation of lipid droplets in *APOE4* astrocytes as compared to *APOE3* astrocytes (Fig. S1B).

APOE4 alters the lipid burden in microglia

To address whether the *APOE4*-associated intracellular lipid accumulation was present in other cell types, we examined microglia, which play a key role in AD (33) and were recently described to accumulate lipids in aged mice (4). We derived *APOE3* and *APOE4* microglia from our isogenic iPSC lines (Fig. S1C) and measured their lipid droplet content. We observed fewer lipid droplet bearing-microglia in culture than we observed for astrocytes under similar culture conditions. Even so, *APOE4* microglia showed more lipid droplet positive cells per well (Fig. S1E, left panel) than did *APOE3* microglia. Following 2 weeks of culture in minimal media, *APOE4* microglia displayed a trend towards increased lipid droplet numbers per cell when compared to *APOE3* microglia (Fig. S1D). Stimulation of the cultures by interferon gamma resulted in increased numbers of lipid droplet bearing cells for both *APOE3* and *APOE4* cells (Fig. S1E, right panel). These findings suggest that *APOE4*-associated lipid dysregulation occurred in multiple glial cell types.

Gene expression in brain tissue from individuals with the *APOE4* allele suggests dysregulation in lipid metabolism

To determine whether our iPSC-derived human astrocyte cultures reflected *APOE4*-related dysfunction present in human brains, we examined transcriptomic data from postmortem human brain samples characterized in the Genotype-Tissue Expression (GTEx) project, containing tissue-specific gene expression data for individuals of varying genotype, age, and cause of death. We explored the influence of the *APOE4* allele on lipid metabolic pathways, independent of disease state, by comparing the transcriptomic profiles of *APOE4* carriers to non-carriers across a Kyoto Encyclopedia of Genes and Genomes (KEGG)-based curated set of 609 lipid metabolism genes (Fig. S1F, Table S1); 529 genes were detected within the GTEx cortex dataset. Of the genes that were significantly differentially expressed (False Discovery Rate (FDR) corrected p-value <0.05) in *APOE4* carriers when compared to non-carriers, we identified upregulated genes involved in the metabolism of neutral lipids and cholesterol (*FA2H, ACSL1, SQLE, HMGCR, MVK*), as well as downregulated genes

involved in the metabolism of fatty acids and neutral lipids (*OLAH, CNEP1R1, GPAM)* (Fig. S1F). This analysis suggested that in the human cortex, *APOE4*-mediated perturbation of lipid metabolism could be detected in the transcriptome of *APOE4* carriers.

Expression of APOE4 in yeast recapitulates lipid defects identified in human astrocytes

In order to explore *APOE4*-associated lipid defects in an unbiased and genetically tractable manner, we utilized the remarkable conservation of lipid metabolism pathways across eukaryotes including baker's yeast, *Saccharomyces cerevisiae* (21, 23, 24, 34).

We first established an *APOE* model in yeast that captured the lipid dysfunction that we observed in human cells. Our model used the human cDNA of *APOE3* and *APOE4*, directed to the secretory pathway using the signal sequence from *S. cerevisiae* Kar2p (Fig. S2A), to mirror the localization of APOE in human cells (35, 36). The constructs were driven by tunable transcriptional activation by β-estradiol (37). We found that expression of human *APOE4*, but not human *APOE3*, induced the accumulation of lipid droplets in yeast grown in minimal culture media (Fig. 2A), just as we had observed for *APOE4*-expressing human iPSC-derived astrocytes. The *APOE4* yeast strain also accumulated the lipid droplet-resident proteins, Erg6p and Faa4p (Fig. S2B) (38). Yeast cells expressing other neurodegenerative disease-related proteins, Aβ1-42 and TDP-43, showed only a minor increase in accumulation of the neutral lipid dye, BODIPY 493/503, compared to *APOE4*-expressing yeast (Fig. S2C). The extent of lipid accumulation and dysregulation therefore was a unique feature of *APOE4*-expressing cells.

We performed lipid extraction and lipidomic analyses of *APOE3* and *APOE4*-expressing yeast, observing an increase in levels of triacylglycerides (Fig. 2B) and the unsaturated fatty acids attached to them (Fig. S2D), similar to what we observed in *APOE4*-expressing human iPSC-derived astrocytes. Thus, expression of *APOE4* in our yeast model induced similar lipid defects to those observed in iPSC-derived astrocytes and therefore could be used to probe the genetics underlying this effect.

Loss-of-function genetic screens in yeast reveal genetic suppressors of APOE4-mediated lipid defects

The disruption in lipid homeostasis in *APOE4*-expressing yeast was accompanied by an isoform-specific growth defect when the yeast were grown on either solid media (Fig. 2C) or in liquid synthetic Complete Supplement Mixture media (Fig. 2D, S3A). This growth defect scaled with expression of *APOE4*, where increasing amounts of APOE4 protein correlated with a reduction in the growth rate (Fig. S3B). This effect was not observed for APOE3-expressing yeast (Fig. S3C).

Given that *APOE4*-expressing yeast exhibited the lipid homeostasis defects observed in *APOE4*-expressing human iPSC-derived astrocytes, we performed loss-of-function genetic screens among the non-essential genes in the yeast genome to identify genetic suppressors of the *APOE4*-induced growth phenotype (39, 40). We performed two independent screens with the *APOE4* gene expressed either from a cassette integrated into the yeast genome or from a centromeric plasmid (Fig. S3D). The gene deletion strains that exhibited unperturbed growth despite the expression of *APOE4* (Fig. 2E, S3E) were enriched for genes whose

protein products are associated with the endoplasmic reticulum (Fig. S3F), with many genes reported to genetically interact with each other (41). Our top hits were *OPI1, MGA2* and *UBX2,* which all encode proteins that regulate lipid metabolism (42, 43). Mga2p and Ubx2p act as sensors for fatty acid saturation (42, 44–46) and Opi1p works as a sensor of phospholipid composition (47–49). We focused on *MGA2* and *OPI1* and found that deletion of neither *MGA2* nor *OPI1* altered the amounts of APOE4 protein (Fig. 2G). Given the established role of Mga2p and Opi1p in yeast lipid metabolism (42, 47, 48, 50), our results reaffirm that the *APOE4*-associated growth impediment in yeast stemmed from abnormal lipid metabolism.

An imbalance in lipid saturation is the primary contributor to APOE4-associated lipid defects in yeast

Both Ubx2p and Mga2p control the stability and expression of the only fatty acyl-CoA desaturase in yeast, *OLE1 (42, 51, 52).* Since the Ole1p desaturase is an essential gene in yeast, it was not present in the library we used for our loss-of-function genetic screens. We engineered an *mga2*Δ yeast strain in which *APOE4* expression was no longer associated with a growth defect. We observed that complementation of the *mga2*Δ strains with either *MGA2* or *OLE1* under control of a constitutively active promoter rendered yeast cells sensitive again to *APOE4* expression (Fig. S3G). Chemical inhibition of Ole1p with a small molecule (ECC145) (53), restored the growth of *APOE4*-expressing yeast cells in a dose-dependent manner without impacting the growth of *GFP*-expressing or *APOE3*-expressing cells (Fig. 3H). Lastly, we asked if *MGA2* is involved in the *APOE4*-mediated accumulation of LDs. We measured the BODIPY 493/503 signal in the *mga2*Δ strain and found that the signal does not accumulate (Fig. 2I).

Lipid droplets act to buffer against lipotoxicity by sequestering free fatty acids (FFAs) as triacylglycerides (54). To test whether a high burden of triacylglycerides altered the lipid buffering capacity of *APOE4*-expressing yeast cells, we treated this strain with oleic acid (C18:1), an unsaturated FFA. We found that whereas the growth of both wildtype and *APOE3*-expressing yeast was not affected by the addition of FFAs, the growth defect in the *APOE4*-expressing yeast was exacerbated by addition of oleic acid (Fig. S3H).

Choline supplementation is sufficient to rescue APOE4-induced lipid defects in yeast

Cellular lipid metabolism is shaped by both the genes and the environment (55). We asked whether yeast media differing in nutrient content could modify the growth of *APOE4*-expressing or *APOE3*-expressing yeast. Whereas yeast grown in synthetic media displayed a growth difference between *APOE3*-expressing and *APOE4*-expressing cells, yeast grown in a rich media (yeast extract-peptone) did not (Fig. S4A, S4B). This observation suggested that the *APOE4* slow-growth phenotype depended on nutrient availability. This effect was specific to APOE4 as other proteins (Aβ1-42, TDP43) displayed a clear growth disadvantage in both synthetic media and yeast extract-peptone (YP) media (Fig. S4A). This finding suggested that environmental factors could modify *APOE4* phenotypes in yeast.

Given that one of our top genetic screen hits, *OPI1* is a negative regulator of phospholipid synthesis (48, 49, 56), we asked whether the soluble precursors of phospholipid synthesis,

ethanolamine and choline (57), could modulate the *APOE4*-related growth defect (58). While ethanolamine did not influence growth of yeast expressing *APOE4*, addition of choline salts (choline chloride or choline bitartrate) to synthetic yeast media was sufficient to suppress the *APOE4*-associated growth defect (Fig. 3A) in a dose-dependent manner (Fig. 3B). Similar to the genetic rescue observed upon deletion of *MGA2*, choline supplementation did not simply decrease APOE4 protein (Fig. 3C), but rather uncoupled the presence of APOE4 from its growth-perturbing effects. Furthermore, the observed rescue was specific to *APOE4*, as synthetic medium supplemented with choline did not rescue the growth defect in yeast expressing Aβ1-42 (Fig. S4C). Given that choline is a growth-limiting factor in *APOE4*-expressing yeast cultured in synthetic medium, we measured intracellular levels of choline and the choline derivatives, phosphocholine and glycerophosphocholine. We found that, compared to *APOE3*-expressing yeast, *APOE4*-expressing yeast grown in synthetic media contained elevated concentrations of these molecules (Fig. S4D).

Choline (trimethylamine) serves as the head group for phosphatidylcholines and sphingomyelins, and functions as a signaling molecule and methyl donor (59). Both yeast and human cells can generate phosphatidylcholine by the choline-dependent Kennedy pathway or the choline-independent phosphatidylethanolamine methylation pathway (Fig. S4E) (57, 60). To understand which of these biosynthesis pathways was relevant to choline-dependent rescue of the *APOE4* phenotypes, we deleted every enzyme in the phosphatidylcholine synthesis or phosphatidylethanolamine synthesis pathways (57). As expected, the genetic ablation of the phosphatidylethanolamine synthesis pathway did not impact the growth of *APOE3*-expressing or *APOE4*-expressing strains cultured in nutrient-rich yeast extract-peptone media (Fig. S4F). In contrast, the deletion of every enzyme acting in the phosphatidylcholine synthesis pathway rendered *APOE4*-expressing strains slow-growing, despite being grown in the nutrient-rich yeast extract-peptone media (Fig. S4F). We also observed differential growth between *APOE3*-expressing and *APOE4*-expressing strains upon deletion of *HNM1,* a transporter that carries choline and ethanolamine into yeast cells (61). We therefore concluded that without *HNM1, CKI1, PCT1* and *CPT1,* yeast cells could not process the excess choline delivered by the yeast extract-peptone media to support the growth of *APOE4*-expressing yeast. Thus, the Kennedy pathway was necessary to sustain the growth of *APOE4*-expressing yeast.

APOE4-expressing yeast cells show elevated levels of phosphatidylcholine

To characterize the broader impact of choline supplementation on cellular lipid composition, we used LC-MS-based lipidomics to analyze lipids from *APOE3*-expressing and *APOE4*-expressing yeast grown in either synthetic medium alone or synthetic medium supplemented with choline. Along with the previously observed increases in triacylglycerides and unsaturated fatty acids upon *APOE4* expression (Fig. 2B, S2D), *APOE4*-expressing yeast cells also displayed elevated total phosphatidylcholine when cultured in minimal synthetic medium (Fig. S4G). These data suggested that *APOE4*-expressing cells may have engaged the phosphatidylcholine synthesis pathway to provide an alternate sink for unsaturated fatty acids that would otherwise have accumulated in triglycerides and lipid droplets, resulting in an increased requirement for choline. Indeed, choline supplementation decreased both

intracellular triacylglycerides (Fig. 3D) and the quantities of unsaturated fatty acids attached to triacylglycerides in *APOE4*-expressing yeast to levels found in *APOE3*-expressing cells (Fig. 3E). In line with this result, choline supplementation also prevented lipid droplet accumulation in *APOE4*-expressing yeast (Fig. 3F).

Targeting of lipid desaturation and triacylglyceride synthesis modifies APOE4-mediated lipid accumulation in iPSC-derived astrocytes

We then investigated whether our findings in yeast could be reproduced in human iPSC-derived astrocytes. Examining previously published transcriptomes of human iPSC-derived astrocytes (27), we noted that *APOE4*-expressing human iPSC-derived astrocytes showed a decrease in transcripts of fatty acid desaturases including *SCD* and *FADS2* (Fig. S5A), suggesting that, as in yeast, fatty acid saturation enzymes could be mediating *APOE4*-associated lipid defects. We chemically interrogated this pathway by treating *APOE4*-expressing human iPSC-derived astrocytes in culture with a small molecule inhibitor of SCD1 (A939572) (62), the human homolog of yeast Ole1p. Inhibition of SCD1 resulted in a reduced number of lipid droplets (Fig. 4A) analogous to our finding in *APOE4*-expressing yeast (Fig. 2I).

Triacylglyceride and phosphatidylcholine synthesis pathways share a common substrate, diacylglycerol (Fig. S5B). We hypothesized that chemically impairing the synthesis of triacylglycerides so that only diacylglycerol served as a substrate only for the synthesis of phospholipids would ameliorate the lipid droplet burden in *APOE4*-expressing human iPSC-derived astrocytes. We treated *APOE4*-expressing human iPSC-derived astrocytes with small molecule inhibitors of diglyceride acyltransferases 1 and 2 (63, 64), and observed a decrease in the lipid droplet number in the inhibitor-treated astrocytes compared to control untreated astrocytes (Fig. 4B, S5C). Therefore, *APOE4*-associated lipid defects may have arisen from the accumulation of endogenously synthesized lipids. Higher endogenous triacylglycerides and lipid droplet burden also suggested that *APOE4*-expressing human iPSC-derived astrocytes might present a genotype-specific sensitivity to challenge with exogenous lipids, as lipid droplets sequester FFAs into triacylglycerides to prevent lipotoxicity (54). Addition of the unsaturated fatty acid oleic acid to *APOE4*-expressing human iPSC-derived astrocytes in culture exacerbated lipid droplet accumulation (~3-fold) compared to *APOE3*-expressing human iPSC-derived astrocytes (Fig. 4C) (26), suggesting that *APOE4*-expressing human iPSC-derived astrocytes had reduced capacity to buffer excess lipids.

Choline supplementation reverses defective lipid homeostasis in human APOE4-expressing iPSC-derived astrocytes

Having shown that choline-stimulated synthesis of phosphatidylcholine restored lipid metabolism in *APOE4*-expressing yeast, we examined choline derivatives in metabolites extracted from our human iPSC-derived astrocytes. Similar to our observations in yeast, we found an increase in choline and glycerophosphocholine in *APOE4* astrocytes, suggesting an increased demand for uptake of choline and its metabolites (Fig. S5D). Betaine, a choline derivative used in one-carbon metabolism but not in phosphatidylcholine synthesis, did not show changes in abundance between *APOE* genotypes (Fig. S5D) suggesting that

exogenously acquired choline metabolites were preferentially channeled towards phosphatidylcholine synthesis in *APOE4* astrocytes.

We then explored the effect of choline supplementation on *APOE4*-associated lipid perturbations in human iPSC-derived astrocytes *in vitro*. We cultured *APOE3* and *APOE4* isogenic astrocytes in either standard media or media supplemented with cytidine 5'-diphosphocholine (CDP-choline), a direct precursor of phosphatidylcholine synthesis by the Kennedy pathway (65). *APOE4*-expressing astrocytes treated with CDP-choline showed a decrease in lipid droplet number to that found in *APOE3*-expressing astrocytes (Fig. 4D). Further, lipidomic profiling showed that CDP-choline treatment resulted in the reduction of total triacylglycerides in *APOE4* astrocytes (Fig. 4E). CDP-choline treatment also reduced the enrichment of unsaturated fatty acids in *APOE4* astrocytes (Fig. 4F). These results confirmed that choline supplementation ameliorated the *APOE4*-induced lipid defects in iPSC-derived human astrocytes *in vitro*.

Choline supplementation rescues cholesterol accumulation associated with APOE4

Lipid droplets are composed not only of triacylglycerides but also of cholesterol and cholesterol esters (30, 54). Cholesterol regulation plays a key role in *APOE*-related diseases including both cardiovascular disease and AD (3, 66). We previously reported using a fluorescent probe Filipin III (67) that *APOE4* astrocytes accumulate cholesterol (27). Cholesterol metabolism, including biosynthesis, efflux and cholesterol storage in lipid droplets, is tuned to the cholesterol/phosphatidylcholine ratio in mammalian cells (68). We therefore used Filipin III to examine intracellular cholesterol in human iPSC-derived astrocytes treated with CDP-choline or vehicle in vitro. While vehicle-treated *APOE4*-expressing astrocytes accumulated more cellular cholesterol than did *APOE3*-expressing astrocytes, *APOE4* astrocyte cultures supplemented with CDP-choline did not show this defect (Fig. 4G).

Discussion

Relating genetic polymorphisms to their phenotypic outcomes is key to understanding the molecular bases of disease risk and pathogenesis. In this study, we investigated in human iPSC-derived astrocytes the molecular basis of *APOE4*-associated lipid defects including an aberrant accumulation of unsaturated fatty acids and their storage in triglyceride-rich lipid droplets in human iPSC- derived astrocytes. Previous results in astrocytes from mice with human *APOE* targeted replacement showed an increase in lipid droplets associated with the *APOE4* genotype (26). Another study (3) specifically examined the transcriptomic profiles of human iPSC-derived glia, human glia from postmortem AD patient brain tissue, as well as glia from mice with human *APOE* targeted replacement. This study affirmed the central role of *APOE4* in perturbing lipid metabolism pathways in both humans and mice.

In our cellular models, we found several lipid metabolic nodes that potentially could be manipulated to improve lipid regulation in *APOE4*-expressing yeast cells and human iPSC-derived astrocytes. In particular, we discovered that stimulating phosphatidylcholine synthesis via the Kennedy pathway using exogenous choline supplementation was sufficient to reverse the *APOE4*-induced lipid defects in both yeast and astrocytes while not impacting

APOE4 expression. Compromised activity of the Kennedy pathway has been shown to result in accumulation of intracellular fats in humans and in mouse models bearing mutations in the *PCYT1A* gene (69, 70). Interestingly, a genetic polymorphism in the *PEMT* gene that functions in an alternative phosphatidylcholine synthesis pathway has been associated with AD in a Chinese population (71).

A number of *APOE4*-associated diseases have been linked to alterations in glucose and fatty acid metabolism (72, 73). Lipid metabolism is an area of active investigation in research on aging and neurodegenerative diseases (1–4, 6, 27). Indeed, AD-associated intracellular lipid accumulation has been reported in the postmortem brain tissue of AD patients (5), human fibroblasts (74), transgenic mouse models of AD (5), mouse primary culture of neurons (26), and flies (75) expressing *APOE4*.

Many lipid species have been implicated in neurotoxicity or selected as markers for early diagnosis of AD (76). Examination of a number of postmortem AD brains revealed a reduction in choline, ethanolamine, phosphatidylcholine and phosphatidylethanolamine and an increase in their degradation products (77). Our data suggest that the *APOE4* genotype may impose additional choline dependency thus exacerbating the cholinergic deficit found in AD brains. In fact, our analysis of transcriptomes in postmortem brain tissue from *APOE4* carriers revealed that these individuals had increased expression of the high-affinity choline transporter *SLC44A1* (Fig. S1F).

Over the last three decades, the link between age-related cognitive decline and compromised lipid metabolism has been increasingly appreciated. As a result, nutritional interventions aimed at elevating the synthesis of phospholipids became attractive as a noninvasive therapeutic strategy (78, 79). CDP-choline itself has been previously proposed as a dietary supplement (80, 81). In general, the demand for dietary choline may depend on multiple factors like age, ethnicity, and sex (82). For example, women tend to develop choline deficiency more often than do men (65). Intriguingly, women with an *APOE4* genotype show an increased risk of AD (83, 84). Although most clinical trials for choline derivatives supplementation in AD did not stratify individuals by *APOE* genotype, those that did noted greater efficacy of choline supplementation in *APOE4* populations than in those without the *APOE4* genotype (85). Our findings could point to a therapeutic strategy where choline supplementation is targeted to those with the *APOE4* genotype. Given our study is limited to *in vitro* cell models, future research is required to expand the findings in animal models and *APOE4* carriers. For example, it would be interesting to examine how specific dietary changes impact brain metabolites and lipids in *APOE4* models and carriers and whether this impacts progression of *APOE4*-associated diseases. Such lines of research could identify the early-stage biomarkers of *APOE4*-dependent pathological states.

Lipid homeostasis impacts many cellular processes, including membrane synthesis, vesicular trafficking, protein turnover and cell proliferation (86). Our study suggests that *APOE4*'s status as a genetic risk factor for AD and other distinct diseases originates from the pleiotropic consequences of perturbed lipid metabolism characterized by increases in unsaturated triacylglycerides and a higher phosphatidylcholine requirement compared to the *APOE3* genotype. Our work provides a framework for understanding APOE4 function in

disease risk and provides a rationale for genotype-specific dietary supplementation to diminish the detrimental consequences of the *APOE4* genetic polymorphism.

Materials and Methods

The objective of this study was to establish the molecular consequences of the *APOE4* allele in yeast and human iPSC-derived astrocytes *in vitro* and to modulate theses effects using chemical and genetic interventions. The study used *APOE3* and *APOE4* isogenic pairs of human iPSC-derived astrocytes and microglia, and yeast expressing human *APOE4* or *APOE3*. We measured the intracellular lipid content of yeast and human astrocytes using fluorescent probes and mass spectroscopy, and yeast growth after chemical and genetic perturbations. The sample sizes were selected based on previous literature. The number of replications varied and is indicated in each figure legend. The study was not blinded.

Human iPSC-derived cell culture

iPSC-derived lines were generated from the parent line Coriell #AG09173 (female *APOE3/3* parental) and #AG10788 (female APOE4/4 parental). Differentiation into astrocytes was performed as previously described (27). iPSCs were derived into microglia using a previously described protocol (87) with minor modifications.

Lipid droplet analysis

To assay the number of lipid droplets in astrocytes, equal number of cells were plated on the 96-well μ-Plate (Ibidi, 89626) in astrocyte medium or astrocyte medium supplemented with SCD1 inhibitor (A939572, 100nM), inhibitors of DGAT1 (PF-04620110, 1μM) and DGAT2 (PF-06424439, 1μM), or CDP-choline (Sigma-Aldrich, 100μM). After 12-14 days cells were stained with LipidTox (ThermoFisher/Molecular Probes) or Filipin III (Sigma-Aldrich) according to manufacturer's protocols. To induce lipid droplet formation, astrocytes were incubated in the presence of oleic acid (Sigma-Aldrich, 20μM) or vehicle (control). After 6 hours, the cells were carefully washed and stained with LipidTox, and proceeded as above. For lipid droplet count analysis in microglia, cells were plated at a density of 10,000 cells per well in a 96-well glass bottom plate (IBIDI) in iMBM media prepared with custom DMEM/F12 lacking choline (Gibco), and supplemented with a low amount of choline chloride (Sigma-Aldrich, 15 μM). The cells were cultured for two weeks following plating without media changes and were then fixed and stained using LipidTox Red (Thermo Fischer/Molecular Probes).

GTEx transcriptomics analysis

The genotypes of *APOE* ε4 (rs429358) for 838 subjects in the GTEx project (version 8) were extracted from vcf files (hg38) called from whole genome sequencing data. Differential gene expression analysis of *APOE* ε4 (dichotomized into two groups, *APOE* $\varepsilon4^+$ and *APOE* $\varepsilon4^-$) was performed using DESeq2 (88) adjusted for RIN, age, sex and five remove unwanted variation (RUV) components. The mean age of death of the sample is 57.56 +/− 10.34(S.D). 68.8% of the individuals are male, and 89.8% are white.

Yeast

Saccharomyces cerevisiae strains were isogenic to the BY4741 background (MATa *his3Δ1 leu2Δ0 met15Δ0 ura3Δ0*). For the deletion of genes, a PCR product containing a selection cassette and short sequences for site-specific homologous recombination was transformed to yeast as described (89). Yeast were grown with at 30°C in synthetic media (SC) with YNB or nutrient-rich (YP) media supplemented with 2% glucose (or 1% galactose only in Fig. S2A and genetic screens). Yeast growth was measured using Epoch 2 Microplate Spectrophotometer (BioTek) and quantified as an area under the growth curve within the 24 hours post induction (starting at OD 600 nm =0.1).

Ole1p inhibitor ECC145 was produced by ChemBridge Co. (San Diego, CA, USA) and was added at indicated concentrations (10, 20, 40μM) to the synthetic media containing β-estradiol (100nM).

For genetic screens, we expressed APOE variants under galactose-inducible promoter. For screen validations and subsequent follow-up experiments, we adopted β-estradiol-inducible system that is independent on carbon source (37, 90). We utilized this system to express APOE variants, TDP-43 and Aβ1-42. For the vast majority of experiments, we used β-estradiol at the 100 nM concentration, unless stated otherwise (e.g. to elicit a mild growth defect, then 10nM of β-estradiol was applied). All the plasmids used in this study were deposited at Addgene (#78653).

Synthetic Genetic Array (SGA)

Bait strains expressing APOE variants under galactose promoter, either integrated in the *LEU2* locus or on a centromeric plasmid, were engineered in the screening strain y7092 (gift from the Boone laboratory). Screens were performed as previously described (39, 91).

Western blotting

The standard trichloroacetic acid (TCA) precipitation-based method was used to extract protein from yeast. Precipitates were resuspended in HU buffer (8 M urea; 5% SDS; 1mM EDTA; 1,5% DTT; 1% bromophenol blue; 200mM Tris-HCl pH 6,8) and incubated at 70°C for 15 min prior to loading on SDS-PAGE gels. To separate proteins by SDS-PAGE, the 4-12% gradient Bis-Tris NuPAGE gels (Invitrogen) run in MES buffer were used. Gels were transferred to a nitrocellulose membrane using the iBlot2 system (ThermoFisher). Primary antibodies were probed overnight followed by several washing steps and incubation with fluorescent secondary antibodies. Signal was measured using the Li-COR (Odyssey) system. Antibodies used in this study: Anti-APOE (mouse monoclonal E8, Santa Cruz), anti-PGK1 (rabbit polyclonal, ABIN568371), anti-mouse secondary 800CW dye conjugate (LI-COR, 926-32212), anti-rabbit secondary 680CW dye conjugate (LI-COR, 926-68073).

Lipidomics analysis

For lipid analysis, iPSC-derived astrocytes (derived from parental line Coriell #AG09173) were seeded in 10cm dish for 12-14 days and grown in the astrocyte medium with 2% dialyzed FBS and supplemented with vehicle or CDP-choline (100μM). Yeast were grown in synthetic media or synthetic media supplemented with choline chloride (1mM). The

expression of APOE variants was induced with β-estradiol (100nM) for 8 hours. 10 ODs equivalent of yeast were collected, washed twice with ice-cold ammonium bicarbonate, and resuspended in 1ml of ammonium bicarbonate. Zirconia beads (Sigma) were added to mechanically disrupts cells using TissueLyser (Qiagen) (28). For both yeast and astrocytes, lipids were extracted using the Folch method (92).

Cytometry analysis after BODIPY 493/503 staining

Yeast strains were grown to saturation in synthetic media with 2% glucose and subsequently diluted to OD_{600} = 0.1 in the synthetic media containing β-estradiol (100nM) for 8 hours. MACSQuant VYB cytometer with a 96-well plate platform (Miltenyi Biotech) was used to acquire 10,000 events in biological triplicates. The BODIPY 493/503 signal (green fluorescence) was measured with the B1 channel (525/50 filter) and median fluorescence values were calculated. Data was processed using FlowJo (FlowJo LLC).

Fluorescence microscopy

Yeast strains were grown to saturation in synthetic media with 2% glucose, diluted to OD_{600} = 0.1 in the synthetic media containing β-estradiol (100nM) for 8 hours. Cells were diluted to OD_{600} of 0.2 in the same media and transferred to a concanavalin A-coated 96-well plate. All images were acquired using a Nikon Eclipse Ti-E inverted microscope equipped with a Nikon Plan Apo 100x oil objective (NA 1.4) and a CCD camera (Andor technology). For all iPSC-derived cell type imaging, images were acquired using a Nikon Plan Apo 63x oil objective (NA 1.4) using a Nikon Eclipse Ti-E inverted microscope and a CCD camera (Andor technology) or a Zeiss LSM710 inverted confocal microscope with a 40x water immersion objective and Z-stacks with a stack height of 0.5μm. Imaging was analyzed using Imaris (Bitplane) spot counting and area functions.

Statistical Analysis

GraphPad Prism software was used to process data, calculate statistics and prepare graphs. For determining statistical significance, we used the unpaired versions of t-tests, unless stated otherwise. FlowJo was used to process FACS data. Images were processed using Imaris and Fiji (93).

Supplementary Material

Refer to Web version on PubMed Central for supplementary material.

Acknowledgments:

This work is dedicated to our inspiring mentor Susan Lindquist. We thank members of the Lindquist, Tsai, and Sabatini labs for helpful suggestions. We thank Prathapan Thiru for technical assistance with bioinformatics, Yuan-Ta Lin for help with iPSC lines and sharing of transcriptomics data and Jose Valderrain for analysis of large-scale datasets. We thank Daniel Jarosz, David Pincus, Peter Tsvetkov, Justin Rettenmaier, Marcello Maresca, Mohammad Bohlooly, Linda Clayton, and Brooke Bevis for suggestions.

Funding:

GS was supported by an EMBO Fellowship (ALTF 829-2015) and was a HHMI fellow of the Helen Hay Whitney Foundation. PN was supported by the Helen Hay Whitney Foundation, by a NIH/NIA K99 award (AG055697-03) and by the Intramural Research Program of the NIH/NIDDK. NK is an HHMI fellow of the Damon Runyon

Foundation. DMS is supported by an NIH/NCI grant (R01 CA103866). He is an investigator of the Howard Hughes Medical Institute and an American Cancer Society Research Professor. The work in the Lindquist and Tsai labs was supported by the Neurodegeneration Consortium, the Robert A. and Renee E. Belfer Foundation, the Howard Hughes Medical Institute, the Ludwig Family Foundation, support from Kara and Stephen Ross, and NIH grants: RF1 AG048029, RF1 AG062377, U01 NS110453, R01 AG062335 and R01 AG058002 (to L-H. T.). The Genotype-Tissue Expression (GTEx) Project was supported by the Common Fund of the Office of the Director of the NIH, and by NCI, NHGRI, NHLBI, NIDA, NIMH, and NINDS.

References and Notes:

1. Fanning S, Haque A, Imberdis T, Baru V, Barrasa MI, Nuber S, Termine D, Ramalingam N, Ho GPH, Noble T, Sandoe J, Lou Y, Landgraf D, Freyzon Y, Newby G, Soldner F, Terry-Kantor E, Kim TE, Hofbauer HF, Becuwe M, Jaenisch R, Pincus D, Clish CB, Walther TC, Farese RV, Srinivasan S, Welte MA, Kohlwein SD, Dettmer U, Lindquist S, Selkoe D, Lipidomic Analysis of α-Synuclein Neurotoxicity Identifies Stearoyl CoA Desaturase as a Target for Parkinson Treatment, Mol. Cell 73, 1001–1014.e8 (2019). [PubMed: 30527540]
2. Shimabukuro MK, Langhi LGP, Cordeiro I, Brito JM, Batista CMDC, Mattson MP, De Mello Coelho V, Lipid-laden cells differentially distributed in the aging brain are functionally active and correspond to distinct phenotypes, Sci. Rep 6, 1–12 (2016). [PubMed: 28442746]
3. Tcw J, Liang SA, Qian L, Pipalia NH, Chao MJ, Shi Y, Bertelsen SE, Kapoor M, Marcora E, Sikora E, Holtzman DM, Maxfield FR, Zhang B, Wang M, Poon WW, Goate AM, Goate AM, Cholesterol and matrisome pathways dysregulated in human APOE E4 glia, bioRxiv 4, 713362 (2019).
4. Marschallinger J, Iram T, Zardeneta M, Lee SE, Lehallier B, Haney MS, V Pluvinage J, Mathur V, Hahn O, Morgens DW, Kim J, Tevini J, Felder TK, Wolinski H, Bertozzi CR, Bassik MC, Aigner L, Wyss-Coray T, Lipid-droplet-accumulating microglia represent a dysfunctional and proinflammatory state in the aging brain, Nat. Neurosci 23, 194–208 (2020). [PubMed: 31959936]
5. Hamilton LK, Dufresne M, Joppé SE, Petryszyn S, Aumont A, Calon F, Barnabé-Heider F, Furtos A, Parent M, Chaurand P, Fernandes KJL, Aberrant Lipid Metabolism in the Forebrain Niche Suppresses Adult Neural Stem Cell Proliferation in an Animal Model of Alzheimer's Disease, Cell Stem Cell 17, 397–411 (2015). [PubMed: 26321199]
6. Alzheimer A, Stelzmann RA, Schnitzlein HN, Murtagh FR, An English translation of Alzheimer's 1907 paper, "Uber eine eigenartige Erkankung der Hirnrinde"., Clin. Anat 8, 429–31 (1995). [PubMed: 8713166]
7. Innerarity TL, Mahley RW, Enhanced binding by cultured human fibroblasts of apo-E-containing lipoproteins as compared with low density lipoproteins., Biochemistry 17, 1440–7 (1978). [PubMed: 206278]
8. Mahley RW, Bersot TP, Lequire VS, Levy RI, Windmueller HG, Brown WV, Identity of Very Low Density Lipoprotein Apoproteins of Plasma and Liver Golgi Apparatus, Science (80-.). 168, 380–382 (1970).
9. Mahley RW, Apolipoprotein E : Cholesterol Transport, Science (80-.). 240, 622–630 (1988).
10. McIntosh AM, Bennett C, Dickson D, Anestis SF, Watts DP, Webster TH, Fontenot MB, Bradley BJ, The apolipoprotein E (APOE) gene appears functionally monomorphic in chimpanzees (Pan troglodytes)., PLoS One 7, e47760 (2012). [PubMed: 23112842]
11. Lambert JC, Heath S, Even G, Campion D, Sleegers K, Hiltunen M, Combarros O, Zelenika D, Bullido MJ, Tavernier B, Letenneur L, Bettens K, Berr C, Pasquier F, Fiévet N, Barberger-Gateau P, Engelborghs S, De Deyn P, Mateo I, Franck A, Helisalmi S, Porcellini E, Hanon O, De Pancorbo MM, Lendon C, Dufouil C, Jaillard C, Leveillard T, Alvarez V, Bosco P, Mancuso M, Panza F, Nacmias B, Boss P, Piccardi P, Annoni G, Seripa D, Galimberti D, Hannequin D, Licastro F, Soininen H, Ritchie K, Blanché H, Dartigues JF, Tzourio C, Gut I, Van Broeckhoven C, Alpérovitch A, Lathrop M, Amouyel P, Arosio B, Coto E, Del Zompo M, Deramecourt V, Epelbaum J, Forti P, Brice A, Ferri R, Scarpini E, Siciliano G, Solfrizzi V, Sorbi S, Spalletta G, Ravaglia G, Sahel J, Valdivieso F, Vepsäläinen S, Pilotto A, Genome-wide association study identifies variants at CLU and CR1 associated with Alzheimer's disease, Nat. Genet 41, 1094–1099 (2009). [PubMed: 19734903]
12. Farrer LA, Cupples LA, Haines JL, Hyman B, a Kukull W, Mayeux R, Myers RH, Pericak-Vance MA, Risch N, van Duijn CM, Effects of age, sex, and ethnicity on the association between

apolipoprotein E genotype and Alzheimer disease. A meta-analysis. APOE and Alzheimer Disease Meta Analysis Consortium., JAMA 278, 1349–1356 (1997). [PubMed: 9343467]

13. Roses AD, M.D, Apolipoprotein E Alleles As Risk Factors in Alzheimer'S Disease, Annu. Rev. Med 47, 387–400 (1996). [PubMed: 8712790]
14. Davignon J, Gregg RE, Sing CF, Apolipoprotein E polymorphism and atherosclerosis, Arterioscler. Thromb. Vasc. Biol 8, 1–21 (1988).
15. Sing CF, Moll PP, Genetics of Variability of CHD Risk, Int. J. Epidemiol 18, S183–S195 (1989). [PubMed: 2807701]
16. Torres-Perez E, Ledesma M, Garcia-Sobreviela MP, Leon-Latre M, Arbones-Mainar JM, Apolipoprotein E4 association with metabolic syndrome depends on body fatness, Atherosclerosis 245, 35–42 (2016). [PubMed: 26691908]
17. Wright KM, Rand KA, Kermany A, Noto K, Curtis D, Garrigan D, Slinkov D, Dorfman I, Granka JM, Byrnes J, Myres N, Ball CA, Ruby JG, A Prospective Analysis of Genetic Variants Associated with Human Lifespan., G3 (Bethesda). 9, 2863–2878 (2019). [PubMed: 31484785]
18. Corder EH, Saunders AM, Strittmatter WJ, Schmechel DE, Gaskell PC, Small GW, Roses AD, Haines JL, Pericak-Vance MA, Gene dose of apolipoprotein E type 4 allele and the risk of Alzheimer's disease in late onset families., Science 261, 921–3 (1993). [PubMed: 8346443]
19. Zhao N, Liu CC, Qiao W, Bu G, Apolipoprotein E, Receptors, and Modulation of Alzheimer's Disease, Biol. Psychiatry 83, 347–357 (2017). [PubMed: 28434655]
20. Zhang Y, Sloan SA, Clarke LE, Caneda C, Plaza CA, Blumenthal PD, Vogel H, Steinberg GK, Edwards MSB, Li G, Duncan JA, Cheshier SH, Shuer LM, Chang EF, Grant GA, Gephart MGH, Barres BA, Purification and Characterization of Progenitor and Mature Human Astrocytes Reveals Transcriptional and Functional Differences with Mouse., Neuron 89, 37–53 (2016). [PubMed: 26687838]
21. Petranovic D, Tyo K, Vemuri GN, Nielsen J, Prospects of yeast systems biology for human health: Integrating lipid, protein and energy metabolism, FEMS Yeast Res. 10, 1046–1059 (2010). [PubMed: 20977625]
22. Khurana V, Lindquist S, Modelling neurodegeneration in Saccharomyces cerevisiae: Why cook with baker's yeast?, Nat. Rev. Neurosci 11, 436–449 (2010). [PubMed: 20424620]
23. Kachroo AH, Laurent JM, Yellman CM, Meyer AG, Wilke CO, Marcotte EM, Systematic humanization of yeast genes reveals conserved functions and genetic modularity, Science (80-.). 348, 921–925 (2015).
24. Natter K, Kohlwein SD, Yeast and cancer cells - Common principles in lipid metabolismBiochim. Biophys. Acta - Mol. Cell Biol. Lipids (2013), doi:10.1016/j.bbalip.2012.09.003.
25. Boyles JK, Pitas RE, Wilson E, Mahley RW, Taylor JM, Apolipoprotein E associated with astrocytic glia of the central nervous system and with nonmyelinating glia of the peripheral nervous system., J. Clin. Invest 76, 1501–13 (1985). [PubMed: 3932467]
26. Farmer B, Kluemper J, Johnson L, Apolipoprotein E4 Alters Astrocyte Fatty Acid Metabolism and Lipid Droplet Formation, Cells 8, 182 (2019).
27. Lin YT, Seo J, Gao F, Feldman HM, Wen HL, Penney J, Cam HP, Gjoneska E, Raja WK, Cheng J, Rueda R, Kritskiy O, Abdurrob F, Peng Z, Milo B, Yu CJ, Elmsaouri S, Dey D, Ko T, Yankner BA, Tsai LH, APOE4 Causes Widespread Molecular and Cellular Alterations Associated with Alzheimer's Disease Phenotypes in Human iPSC-Derived Brain Cell Types, Neuron 98, 1141–1154.e7 (2018). [PubMed: 29861287]
28. Knittelfelder OL, Kohlwein SD, Lipid extraction from yeast cells, Cold Spring Harb. Protoc 2017, 408–411 (2017).
29. Ejsing CS, Sampaio JL, Surendranath V, Duchoslav E, Ekroos K, Klemm RW, Simons K, Shevchenko A, Global analysis of the yeast lipidome by quantitative shotgun mass spectrometry., Proc. Natl. Acad. Sci. {U.S.A.} 106, 2136–2141 (2009). [PubMed: 19174513]
30. Walther TC, Chung J, V Farese R, Lipid Droplet Biogenesis., Annu. Rev. Cell Dev. Biol 33, 491–510 (2017). [PubMed: 28793795]
31. Fam TK, Klymchenko AS, Collot M, Recent Advances in Fluorescent Probes for Lipid Droplets., Mater. (Basel, Switzerland) 11 (2018), doi:10.3390/ma11091768.

32. Straub BK, Gyoengyoesi B, Koenig M, Hashani M, Pawella LM, Herpel E, Mueller W, Macher-Goeppinger S, Heid H, Schirmacher P, Adipophilin/perilipin-2 as a lipid droplet-specific marker for metabolically active cells and diseases associated with metabolic dysregulation, Histopathology 62, 617–631 (2013). [PubMed: 23347084]
33. V Hansen D, Hanson JE, Sheng M, Microglia in Alzheimer's disease., J. Cell Biol 217, 459–472 (2018). [PubMed: 29196460]
34. Singh P, Budding Yeast: An Ideal Backdrop for In vivo Lipid Biochemistry, Front. Cell Dev. Biol 4, 1–8 (2017).
35. Mahley RW, Rall SC, Apolipoprotein E: far more than a lipid transport protein., Annu. Rev. Genomics Hum. Genet 1, 507–37 (2000). [PubMed: 11701639]
36. Treusch S, Hamamichi S, Goodman JL, Matlack KES, Chung CY, Baru V, Shulman JM, Parrado A, Bevis BJ, Valastyan JS, Han H, Lindhagen-Persson M, Reiman EM, Evans DA, Bennett DA, Olofsson A, DeJager PL, Tanzi RE, Caldwell KA, Caldwell GA, Lindquist S, Functional links between Aβ toxicity, endocytic trafficking, and Alzheimer's disease risk factors in yeast, Science (80-.). 334, 1241–1245 (2011).
37. Aranda-Díaz A, Mace K, Zuleta I, Harrigan P, El-Samad H, Robust Synthetic Circuits for Two-Dimensional Control of Gene Expression in Yeast., ACS Synth. Biol 6, 545–554 (2017). [PubMed: 27930885]
38. Athenstaedt K, Zweytick D, Jandrositz A, Kohlwein SD, Daum G, Identification and characterization of major lipid particle proteins of the yeast Saccharomyces cerevisiae., J. Bacteriol 181, 6441–8 (1999). [PubMed: 10515935]
39. Tong AHY, Evangelista M, Parsons AB, Xu H, Bader GD, Pagé N, Robinson M, Raghibizadeh S, V Hogue CW, Bussey H, Andrews B, Tyers M, Boone C, Systematic genetic analysis with ordered arrays of yeast deletion mutants, Science (80-.). 294, 2364–2368 (2001).
40. Giaever G, Chu AM, Ni L, Connelly C, Riles L, Véronneau S, Dow S, Lucau-Danila A, Anderson K, André B, Arkin AP, Astromoff A, El Bakkoury M, Bangham R, Benito R, Brachat S, Campanaro S, Curtiss M, Davis K, Deutschbauer A, Entian KD, Flaherty P, Foury F, Garfinkel DJ, Gerstein M, Gotte D, Güldener U, Hegemann JH, Hempel S, Herman Z, Jaramillo DF, Kelly DE, Kelly SL, Kötter P, LaBonte D, Lamb DC, Lan N, Liang H, Liao H, Liu L, Luo C, Lussier M, Mao R, Menard P, Ooi SL, Revuelta JL, Roberts CJ, Rose M, Ross-Macdonald P, Scherens B, Schimmack G, Shafer B, Shoemaker DD, Sookhai-Mahadeo S, Storms RK, Strathern JN, Valle G, Voet M, Volckaert G, yun Wang C, Ward TR, Wilhelmy J, Winzeler EA, Yang Y, Yen G, Youngman E, Yu K, Bussey H, Boeke JD, Snyder M, Philippsen P, Davis RW, Johnston M, Functional profiling of the Saccharomyces cerevisiae genome, Nature 418, 387–391 (2002). [PubMed: 12140549]
41. Costanzo M, VanderSluis B, Koch EN, Baryshnikova A, Pons C, Tan G, Wang W, Usaj M, Hanchard J, Lee SD, Pelechano V, Styles EB, Billmann M, Van Leeuwen J, Van Dyk N, Lin ZY, Kuzmin E, Nelson J, Piotrowski JS, Srikumar T, Bahr S, Chen Y, Deshpande R, Kurat CF, Li SC, Li Z, Usaj MM, Okada H, Pascoe N, Luis BJS, Sharifpoor S, Shuteriqi E, Simpkins SW, Snider J, Suresh HG, Tan Y, Zhu H, Malod-Dognin N, Janjic V, Przulj N, Troyanskaya OG, Stagljar I, Xia T, Ohya Y, Gingras AC, Raught B, Boutros M, Steinmetz LM, Moore CL, Rosebrock AP, Caudy AA, Myers CL, Andrews B, Boone C, A global genetic interaction network maps a wiring diagram of cellular function, Science (80-.). 353 (2016), doi:10.1126/science.aaf1420.
42. Surma MA, Klose C, Peng D, Shales M, Mrejen C, Stefanko A, Braberg H, Gordon DE, Vorkel D, Ejsing CS, Farese R, Simons K, Krogan NJ, Ernst R, A lipid E-MAP identifies Ubx2 as a critical regulator of lipid saturation and lipid bilayer stress, Mol. Cell 51, 519–530 (2013). [PubMed: 23891562]
43. Schuldiner M, Collins SR, Thompson NJ, Denic V, Bhamidipati A, Punna T, Ihmels J, Andrews B, Boone C, Greenblatt JF, Weissman JS, Krogan NJ, Exploration of the function and organization of the yeast early secretory pathway through an epistatic miniarray profile, Cell 123, 507–519 (2005). [PubMed: 16269340]
44. Covino R, Ballweg S, Stordeur C, Michaelis JB, Puth K, Wernig F, Bahrami A, Ernst AM, Hummer G, Ernst R, A Eukaryotic Sensor for Membrane Lipid Saturation, Mol. Cell (2016), doi:10.1016/j.molcel.2016.05.015.

45. Wang C-W, Lee S-C, The ubiquitin-like (UBX)-domain-containing protein Ubx2/Ubxd8 regulates lipid droplet homeostasis, J. Cell Sci 125, 2930–2939 (2012). [PubMed: 22454508]

46. Kolawa N, Sweredoski MJ, Graham RLJ, Oania R, Hess S, Deshaies RJ, Perturbations to the Ubiquitin Conjugate Proteome in Yeast Δ ubx Mutants Identify Ubx2 as a Regulator of Membrane Lipid Composition, Mol. Cell. Proteomics 12, 2791–2803 (2013). [PubMed: 23793018]

47. Hofbauer HF, Schopf FH, Schleifer H, Knittelfelder OL, Pieber B, Rechberger GN, Wolinski H, Gaspar ML, Kappe CO, Stadlmann J, Mechtler K, Zenz A, Lohner K, Tehlivets O, Henry SA, Kohlwein SD, Regulation of gene expression through a transcriptional repressor that senses acyl-chain length in membrane phospholipids., Dev. Cell 29, 729–39 (2014). [PubMed: 24960695]

48. Klig LS, Homann MJ, Carman GM, Henry SA, Coordinate regulation of phospholipid biosynthesis in Saccharomyces cerevisiae: Pleiotropically constitutive opil mutant, J. Bacteriol 162, 1135–1141 (1985). [PubMed: 3888957]

49. Young BP, Shin JJH, Orij R, Chao JT, Li SC, Guan XL, Khong A, Jan E, Wenk MR, Prinz WA, Smits GJ, Loewen CJR, Phosphatidic Acid Is a pH Biosensor That Links Membrane Biogenesis to Metabolism, Science (80-.). 329, 1085–1088 (2010).

50. Burr R, Stewart EV, Shao W, Zhao S, Hannibal-Bach HK, Ejsing CS, Espenshade PJ, Mga2 transcription factor regulates an oxygen-responsive lipid homeostasis pathway in fission yeast, J. Biol. Chem 291, 12171–12183 (2016). [PubMed: 27053105]

51. Chellappa R, Kandasamy P, Oh CS, Jiang Y, Vemula M, Martin CE, The membrane proteins, Spt23p and Mga2p, play distinct roles in the activation of Saccharomyces cerevisiae OLE1 gene expression. Fatty acid-mediated regulation of Mga2p activity is independent of its proteolytic processing into a soluble transcription act, J. Biol. Chem 276, 43548–56 (2001). [PubMed: 11557770]

52. Zhang S, Skalsky Y, Garfinkel DJ, MGA2 or SPT23 is required for transcription of the delta9 fatty acid desaturase gene, OLE1, and nuclear membrane integrity in Saccharomyces cerevisiae., Genetics 151, 473–483 (1999). [PubMed: 9927444]

53. Xu D, Sillaots S, Davison J, Hu W, Jiang B, Kauffman S, Martel N, Ocampo P, Oh C, Trosok S, Veillette K, Wang H, Yang M, Zhang L, Becker J, Martin CE, Roemer T, Chemical genetic profiling and characterization of small-molecule compounds that affect the biosynthesis of unsaturated fatty acids in Candida albicans., J. Biol. Chem 284, 19754–64 (2009). [PubMed: 19487691]

54. Olzmann JA, Carvalho P, Dynamics and functions of lipid droplets., Nat. Rev. Mol. Cell Biol 20, 137–155 (2019). [PubMed: 30523332]

55. Fei W, Shui G, Zhang Y, Krahmer N, Ferguson C, Kapterian TS, Lin RC, Dawes IW, Brown AJ, Li P, Huang X, Parton RG, Wenk MR, Walther TC, Yang H, A role for phosphatidic acid in the formation of “supersized” Lipid droplets, PLoS Genet 7 (2011), doi:10.1371/journal.pgen.1002201.

56. Loewen CJR, Gaspar ML, a Jesch S, Delon C, Ktistakis NT, a Henry S, Levine TP, Phospholipid metabolism regulated by a transcription factor sensing phosphatidic acid., Science (80-.). 304, 1644–1647 (2004).

57. Henry SA, Kohlwein SD, Carman GM, Metabolism and regulation of glycerolipids in the yeast Saccharomyces cerevisiae, Genetics 190, 317–349 (2012). [PubMed: 22345606]

58. Ramirez-Gaona M, Marcu A, Pon A, Guo AC, Sajed T, Wishart NA, Karu N, Feunang YD, Arndt D, Wishart DS, YMDB 2.0: A significantly expanded version of the yeast metabolome database, Nucleic Acids Res. 45, D440–D445 (2017). [PubMed: 27899612]

59. Wurtman RJ, Cansev M, Sakamoto T, Ulus IH, Use of Phosphatide Precursors to Promote Synaptogenesis, Annu. Rev. Nutr 29, 59–87 (2009). [PubMed: 19400698]

60. Ridgway ND, The role of phosphatidylcholine and choline metabolites to cell proliferation and survival, Crit. Rev. Biochem. Mol. Biol 48, 20–38 (2013). [PubMed: 23350810]

61. Fernández-Murray JP, Ngo MH, McMaster CR, Choline transport activity regulates phosphatidylcholine synthesis through choline transporter Hnm1 stability., J. Biol. Chem 288, 36106–15 (2013). [PubMed: 24187140]

62. Xin Z, Zhao H, Serby MD, Liu B, Liu M, Szczepankiewicz BG, Nelson LTJ, Smith HT, Suhar TS, Janis RS, Cao N, Camp HS, Collins CA, Sham HL, Surowy TK, Liu G, Discovery of piperidine-

aryl urea-based stearoyl-CoA desaturase 1 inhibitors., Bioorg. Med. Chem. Lett 18, 4298–302 (2008). [PubMed: 18632269]

63. Futatsugi K, Kung DW, Orr STM, Cabral S, Hepworth D, Aspnes G, Bader S, Bian J, Boehm M, Carpino PA, Coffey SB, Dowling MS, Herr M, Jiao W, Lavergne SY, Li Q, Clark RW, Erion DM, Kou K, Lee K, Pabst BA, Perez SM, Purkal J, Jorgensen CC, Goosen TC, Gosset JR, Niosi M, Pettersen JC, Pfefferkorn JA, Ahn K, Goodwin B, Discovery and Optimization of Imidazopyridine-Based Inhibitors of Diacylglycerol Acyltransferase 2 (DGAT2)., J. Med. Chem 58, 7173–85 (2015). [PubMed: 26349027]
64. Dow RL, Li J-C, Pence MP, Gibbs EM, LaPerle JL, Litchfield J, Piotrowski DW, Munchhof MJ, Manion TB, Zavadoski WJ, Walker GS, McPherson RK, Tapley S, Sugarman E, Guzman-Perez A, DaSilva-Jardine P, Discovery of PF-04620110, a Potent, Selective, and Orally Bioavailable Inhibitor of DGAT-1., ACS Med. Chem. Lett 2, 407–12 (2011). [PubMed: 24900321]
65. Zeisel SH, da Costa K-A, Choline: an essential nutrient for public health., Nutr. Rev 67, 615–23 (2009). [PubMed: 19906248]
66. Gordon DJ, Probstfield JL, Garrison RJ, Neaton JD, Castelli WP, Knoke JD, Jacobs DR, Bangdiwala S, Tyroler HA, High-density lipoprotein cholesterol and cardiovascular disease. Four prospective American studies., Circulation 79, 8–15 (1989). [PubMed: 2642759]
67. Maxfield FR, Wüstner D, Analysis of cholesterol trafficking with fluorescent probes., Methods Cell Biol. 108, 367–93 (2012). [PubMed: 22325611]
68. Lagace TA, Phosphatidylcholine: Greasing the Cholesterol Transport Machinery., Lipid Insights 8, 65–73 (2015). [PubMed: 27081313]
69. Payne F, Lim K, Girousse A, Brown RJ, Kory N, Robbins A, Xue Y, Sleigh A, Cochran E, Adams C, Dev Borman A, Russel-Jones D, Gorden P, Semple RK, Saudek V, O'Rahilly S, Walther TC, Barroso I, Savage DB, Mutations disrupting the Kennedy phosphatidylcholine pathway in humans with congenital lipodystrophy and fatty liver disease., Proc. Natl. Acad. Sci. U. S. A 111, 8901–6 (2014). [PubMed: 24889630]
70. Vance DE, Vance JE, Physiological consequences of disruption of mammalian phospholipid biosynthetic genes, J. Lipid Res 50, S132–S137 (2009). [PubMed: 18955728]
71. Bi XH, Zhao HL, Zhang ZX, Zhang JW, PEMT G523A (V175M) is associated with sporadic Alzheimer's disease in a Chinese population, J. Mol. Neurosci (2012), doi:10.1007/s12031-011-9630-3.
72. Johnson LA, Torres ERS, Impey S, Stevens JF, Raber J, Apolipoprotein E4 and Insulin Resistance Interact to Impair Cognition and Alter the Epigenome and Metabolome, Sci. Rep (2017), doi:10.1038/srep43701.
73. Nuriel T, Angulo SL, Khan U, Ashok A, Chen Q, Figueroa HY, Emrani S, Liu L, Herman M, Barrett G, Savage V, Buitrago L, Cepeda-Prado E, Fung C, Goldberg E, Gross SS, Hussaini SA, Moreno H, Small SA, Duff KE, Neuronal hyperactivity due to loss of inhibitory tone in APOE4 mice lacking Alzheimer's disease-like pathology, Nat. Commun (2017), doi:10.1038/s41467-017-01444-0.
74. Tambini MD, Pera M, Kanter E, Yang H, Guardia-Laguarta C, Holtzman D, Sulzer D, Area-Gomez E, Schon EA, ApoE4 upregulates the activity of mitochondria-associated ER membranes, EMBO Rep. 17, 27–36 (2016). [PubMed: 26564908]
75. Liu L, MacKenzie KR, Putluri N, Maletić-Savatić M, Bellen HJ, The Glia-Neuron Lactate Shuttle and Elevated ROS Promote Lipid Synthesis in Neurons and Lipid Droplet Accumulation in Glia via APOE/D, Cell Metab. 26, 719–737.e6 (2017). [PubMed: 28965825]
76. Mapstone M, Cheema AK, Fiandaca MS, Zhong X, Mhyre TR, Macarthur LH, Hall WJ, Fisher SG, Peterson DR, Haley JM, Nazar MD, Rich SA, Berlau DJ, Peltz CB, Tan MT, Kawas CH, Federoff HJ, Plasma phospholipids identify antecedent memory impairment in older adults, Nat. Med 20, 415–418 (2014). [PubMed: 24608097]
77. Blusztajn JK, Gonzalez-Coviella IL, Logue M, Growdon JH, Wurtman RJ, Levels of phospholipid catabolic intermediates, glycerophosphocholine and glycerophosphoethanolamine, are elevated in brains of Alzheimer's disease but not of Down's syndrome patients, Brain Res. (1990), doi:10.1016/0006-8993(90)90030-F.

78. Ritchie CW, Bajwa J, Coleman G, Hope K, Jones RW, Lawton M, Marven M, Passmore P, Souvenaid (R): a New Approach To Management of Early Alzheimer'S Disease, J. Nutr. Heal. Aging 18, 291–299 (2014).

79. Caccamo A, Huentelman MJ, Naymik M, Dave N, Velazquez R, Winslow W, Tran A, Ferreira E, Oddo S, Piras IS, Maternal choline supplementation ameliorates Alzheimer's disease pathology by reducing brain homocysteine levels across multiple generations, Mol. Psychiatry (2019), doi:10.1038/s41380-018-0322-z.

80. Grieb P, Neuroprotective properties of citicoline: Facts, doubts and unresolved issues, CNS Drugs 28, 185–193 (2014). [PubMed: 24504829]

81. Conant R, Schauss AG, Therapeutic applications of citicoline for stroke and cognitive dysfunction in the elderly: a review of the literature., Altern. Med. Rev 9, 17–31 (2004). [PubMed: 15005642]

82. Da Costa KA, Corbin KD, Niculescu MD, Galanko JA, Zeisel SH, Identification of new genetic polymorphisms that alter the dietary requirement for choline and vary in their distribution across ethnic and racial groups, FASEB J. 28, 2970–2978 (2014). [PubMed: 24671709]

83. Neu SC, Pa J, Kukull W, Beekly D, Kuzma A, Gangadharan P, Wang LS, Romero K, Arneric SP, Redolfi A, Orlandi D, Frisoni GB, Au R, Devine S, Auerbach S, Espinosa A, Boada M, Ruiz A, Johnson SC, Koscik R, Wang JJ, Hsu WC, Chen YL, Toga AW, Apolipoprotein E genotype and sex risk factors for Alzheimer disease: A meta-analysis, JAMA Neurol. 74, 1178–1189 (2017). [PubMed: 28846757]

84. Damoiseaux JS, Seeley WW, Zhou J, Shirer WR, Coppola G, Karydas A, Rosen HJ, Miller BL, Kramer JH, Greicius MD, Gender Modulates the APOE 4 Effect in Healthy Older Adults: Convergent Evidence from Functional Brain Connectivity and Spinal Fluid Tau Levels, J. Neurosci 32, 8254–8262 (2012). [PubMed: 22699906]

85. Alvarez XA, Mouzo R, Pichel V, Pérez P, Laredo M, Fernández-Novoa L, Corzo L, Zas R, Alcaraz M, Secades JJ, Lozano R, Cacabelos R, Double-blind placebo-controlled study with citicoline in APOE genotyped Alzheimer's disease patients. Effects on cognitive performance, brain bioelectrical activity and cerebral perfusion., Methods Find. Exp. Clin. Pharmacol 21, 633–44 (1999). [PubMed: 10669911]

86. Harayama T, Riezman H, Understanding the diversity of membrane lipid composition., Nat. Rev. Mol. Cell Biol 19, 281–296 (2018). [PubMed: 29410529]

87. McQuade A, Coburn M, Tu CH, Hasselmann J, Davtyan H, Blurton-Jones M, Development and validation of a simplified method to generate human microglia from pluripotent stem cells., Mol. Neurodegener 13, 67 (2018). [PubMed: 30577865]

88. Love MI, Huber W, Anders S, Moderated estimation of fold change and dispersion for RNA-seq data with DESeq2., Genome Biol. 15, 550 (2014). [PubMed: 25516281]

89. Janke C, Magiera MM, Rathfelder N, Taxis C, Reber S, Maekawa H, Moreno-Borchart A, Doenges G, Schwob E, Schiebel E, Knop M, A versatile toolbox for PCR-based tagging of yeast genes: new fluorescent proteins, more markers and promoter substitution cassettes., Yeast 21, 947–62 (2004). [PubMed: 15334558]

90. McIsaac RS, Oakes BL, Wang X, Dummit KA, Botstein D, Noyes MB, Synthetic gene expression perturbation systems with rapid, tunable, single-gene specificity in yeast., Nucleic Acids Res. 41, e57 (2013). [PubMed: 23275543]

91. Kuzmin E, Costanzo M, Andrews B, Boone C, Synthetic genetic array analysis, Cold Spring Harb. Protoc 2016, 359–372 (2016).

92. FOLCH J, LEES M, SLOANE STANLEY GH, A simple method for the isolation and purification of total lipides from animal tissues., J. Biol. Chem 226, 497–509 (1957). [PubMed: 13428781]

93. Schindelin J, Arganda-Carreras I, Frise E, Kaynig V, Longair M, Pietzsch T, Preibisch S, Rueden C, Saalfeld S, Schmid B, Tinevez J-Y, White DJ, Hartenstein V, Eliceiri K, Tomancak P, Cardona A, Fiji: an open-source platform for biological-image analysis., Nat. Methods 9, 676–82 (2012). [PubMed: 22743772]

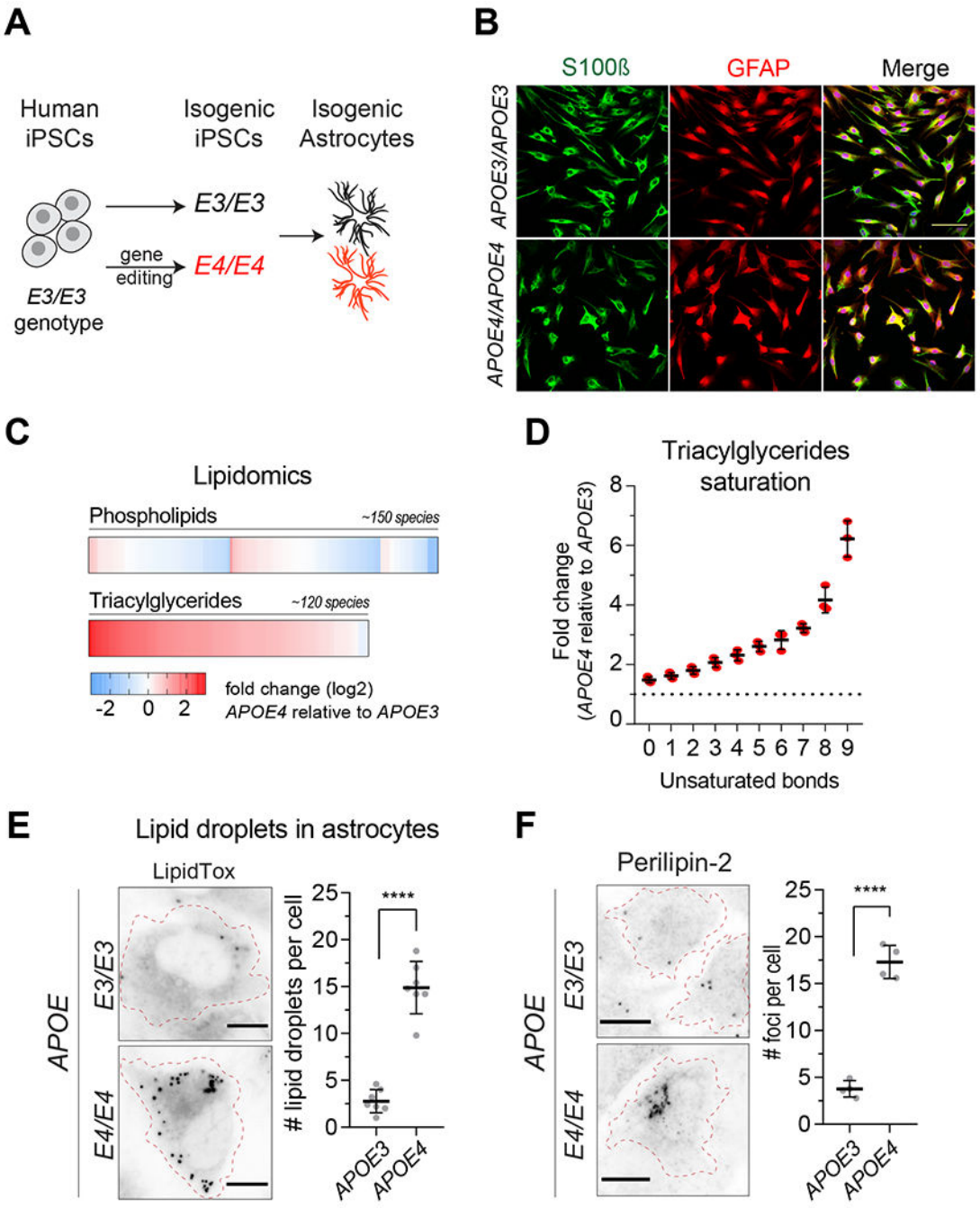

Fig. 1. Increase in lipid droplets in APOE4 human iPSC-derived astrocytes.

(**A**) The schematic shows the differentiation of isogenic astrocytes of the *APOE3/APOE3* and *APOE4/APOE4* genotypes from human iPSCs. (**B**) Representative fluorescence microscopy images (n=3 replicates) of *APOE3/APOE3* and *APOE4/APOE4* isogenic astrocytes stained with antibodies against S100β and GFAP (scale bar 100 μm). (**C**) A heatmap showing the fold change (log2) in abundance of phospholipids (~150 lipid species) and triacylglycerides (~120 species) between isogenic *APOE4/APOE4* and *APOE3/APOE3* human iPSC-derived astrocytes. (**D**) Graph shows fold change difference in the number of

unsaturated bonds in fatty acids attached to triacylglycerides between isogenic *APOE4/APOE4* and *APOE3/APOE3* human iPSC-derived astrocytes. For this analysis, we summed the number of unsaturated carbon bonds per triacylglyceride molecule. (**E**) Representative microscopy images of isogenic *APOE4/APOE4* and *APOE3/APOE3* human iPSC-derived astrocytes in culture stained with LipidTox. Quantification of the lipid droplet number per cell is shown in the right panel, with each dot representing an average of at least 20 cells in four wells analyzed (n=7 independent replicates). Data are represented as mean ± SD; **** $p \leq 0.0001$ by Student's t-test. The dashed line denotes the boundaries of the cell (scale bar, 20 μm). (**F**) Representative microscopy images of isogenic *APOE4/APOE4* and *APOE3/APOE3* human iPSC-derived astrocytes in culture stained with an anti-Perilipin 2 antibody. Magnification is the same as in (E). Quantification of the Perilipin-2 foci per cell is shown in the right panel, with each dot representing an average of four wells with at least 20 cells analyzed (n=4 independent replicates). Data are represented as mean ± SD ; **** $p \leq 0.0001$ by Student's t-test.

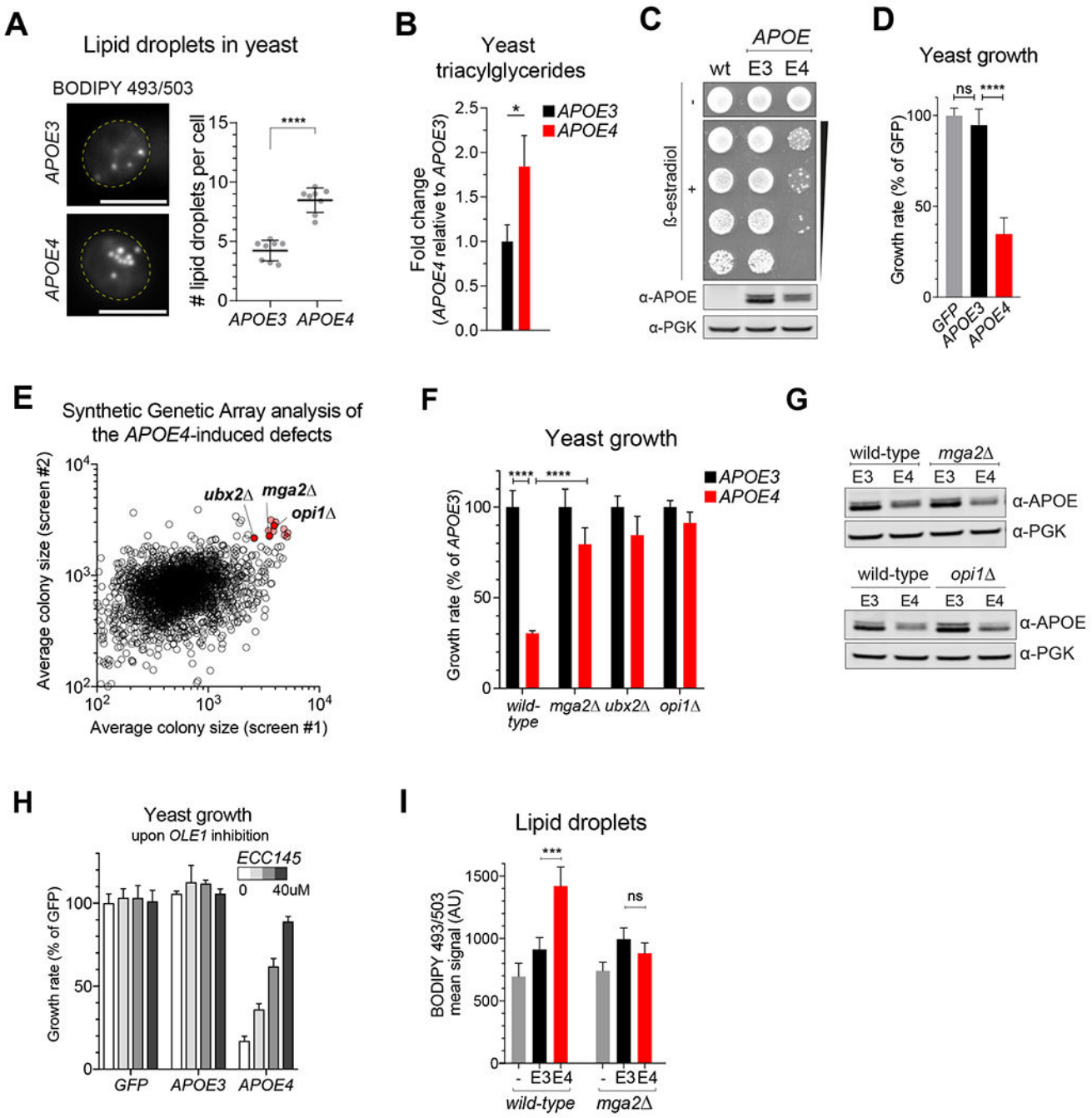

Fig. 2. Lipid homeostasis is perturbed in yeast expressing human *APOE4*.

(**A**) Representative fluorescence microscopy images of yeast expressing human *APOE3* or *APOE4* stained with BODIPY 493/503 stain for lipid droplets after growth in synthetic medium (scale bar, 5 μm). Quantification of the number of lipid droplets in yeast is shown in the right panel (n=8 experiments, each with at least 30 yeast cells analyzed). Data are represented as mean ± SD; **** $p \leq 0.0001$ by Student's t-test. The dashed line denotes the boundaries of the yeast cell. (**B**) Bar graph shows fold change difference in intracellular triacylglycerides between *APOE3*-expressing and *APOE4*-expressing yeast cells. Data

representsmean ± SD, n=2 independently grown colonies. * $p \leq 0.05$ by Student's t-test. (**C**) Shown is a yeast growth assay on agar plates containing synthetic complete medium with (+) or without (−) β-estradiol to induce the expression of human *APOE3* or *APOE4*. Representative agar plate shows 5-fold dilutions of yeast cultures. Western blot shows yeast samples collected from the agar plate after 8 hours of β-estradiol induction of *APOE3* or *APOE4* expression. APOE3 and APOE4 were probed with anti-APOE antibody; anti-PGK1 antibody was used as a loading control. (**D**) Bar graph shows growth of wildtype yeast expressing *GFP* or yeast expressing human *APOE3* or *APOE4* cultured in synthetic complete medium for 24 hours. Data are normalized to the growth rate of the GFP-expressing strain (control) and represented as mean ± SD, n=3 independent yeast colonies with at least two technical replicates. ns, nonsignificant $p > 0.05$; **** $p \leq 0.0001$ by Student's t-test. (**E**) A scatter plot from two independent loss-of-function screens showing the average colony size of yeast deletion strains with loss of individual non-essential genes and expressing human *APOE4*. Each circle represents data averaged from four technical replicates. Yeast strains with variability higher than SD>25% between technical replicates were removed resulting in ~2800 genes assayed). (**F**) Bar graph shows the growth of yeast expressing *APOE4* compared to those expressing *APOE3* for a wildtype strain and *mga2Δ, ubx2Δ and opi1Δ strains*. Data are represented as mean ± SD, n=3 independent yeast colonies with at least two technical replicates each. $p \leq 0.05$; **** $p \leq 0.0001$. (**G**) A Western blot of whole cell extracts of wildtype and *MGA2*-null yeast (top) and wildtype and *OPI1*-null yeast (bottom) showing expression of human APOE3 and APOE4, with PGK1 as loading control. (**H**) Bar graph shows the growth rate of *APOE3*-expressing and *APOE4*-expressing yeast treated with 10, 20 or 40 μM of ECC145 (an Ole1p inhibitor) or vehicle (DMSO). The data are normalized to the growth of a control untreated yeast strain expressing GFP. Data are represented as mean ± SD, n=3 independent yeast colonies with at least two technical replicates each). (**I**) Bar graph shows the mean signal of BODIPY 498/503 staining measured by fluorescence-based cell cytometry in yeast expressing human *APOE3* or *APOE4* for a wildtype strain or a *MGA2*-null strain. Data represent mean ± SD, n=3 independent yeast colonies with at least two technical replicates each. *** $p \leq 0.001$ by Student's t-test.

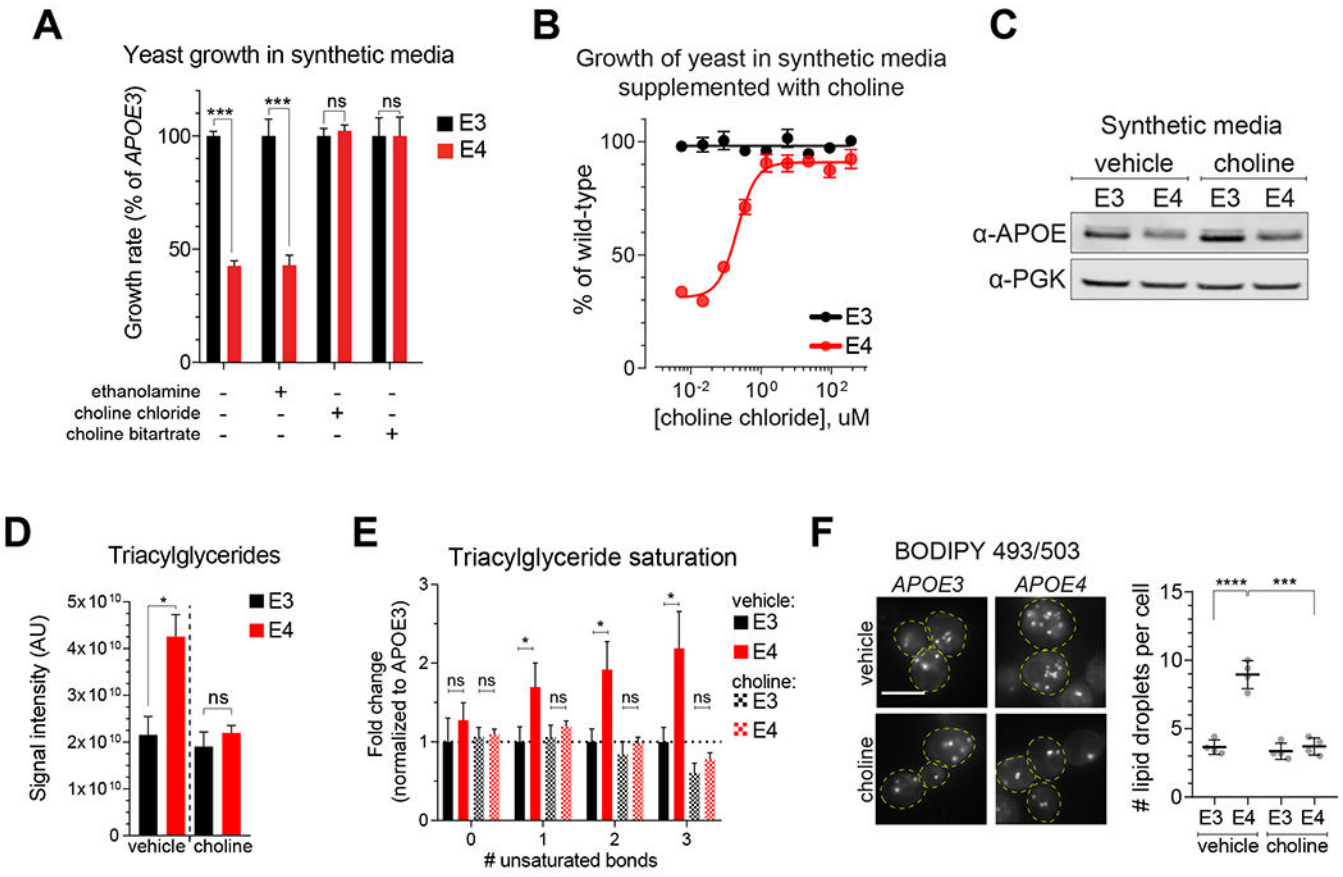

Fig. 3. Choline supplementation rescues *APOE4*-mediated lipid defects in yeast.

(**A**) Shown is relative growth of *APOE4*-expressing yeast in synthetic media supplemented with ethanolamine (1 mM), choline chloride (1 mM) or choline bitartrate (100 μg/ml). Data are shown relative to the growth of the *APOE3*-expressing strain. Data are represented as mean ± SD, n=3 independent yeast colonies with at least two technical replicates each. ns, nonsignificant $p > 0.05$; *** $p \leq 0.001$, Student's t-test. (**B**) Graph shows growth of *APOE4*-expressing and *APOE3*-expressing yeast strains normalized to a wildtype strain after culture in synthetic media supplemented with choline chloride. Data represent measurements of three independent yeast colonies with at least two technical replicates each. (**C**) Western blot of whole cell extracts of yeast expressing *APOE3* or *APOE4* cultured in synthetic media with or without choline supplementation (1 mM), with PGK1 serving as loading control. (**D**) Bar graph shows intracellular triacylglycerides in *APOE3*-expressing and *APOE4*-expressing yeast cells grown in synthetic media with choline (1 mM) supplementation (square pattern) or vehicle (fill) as control. Data represent mean ± SD, n=3 independent yeast colonies. ns, nonsignificant $p > 0.05$; * $p \leq 0.05$ by Student's t-test. (**E**) Bar graph shows the fold change difference in intracellular triacylglycerides in *APOE3*-expressing and *APOE4*-expressing yeast cells grown in synthetic medium supplemented with choline (1mM) or vehicle as control. Triacylglycerides were stratified by the total number of unsaturated bonds present in the attached fatty acids. Data represent mean ± SD, n=3 independent yeast colonies measured. ns nonsignificant $p > 0.05$; * $p \leq 0.05$ by Student's t-test. (**F**) Representative fluorescence microscopy images of *APOE3*-expressing and *APOE4*-

expressing yeast stained with BODIPY 493/503 stain for lipid droplets after growth in synthetic media supplemented with choline (1mM) or vehicle as control. Scale bar, 5μm. Dashed yellow lines demarcate individual yeast cells. Quantification of the number of lipid droplets is shown in the right panel (n=4 experiments, each with at least 30 yeast cells analyzed). Data are represented as mean ± SD , *** $p \leq 0.001$, **** $p \leq 0.0001$ by ANOVA.

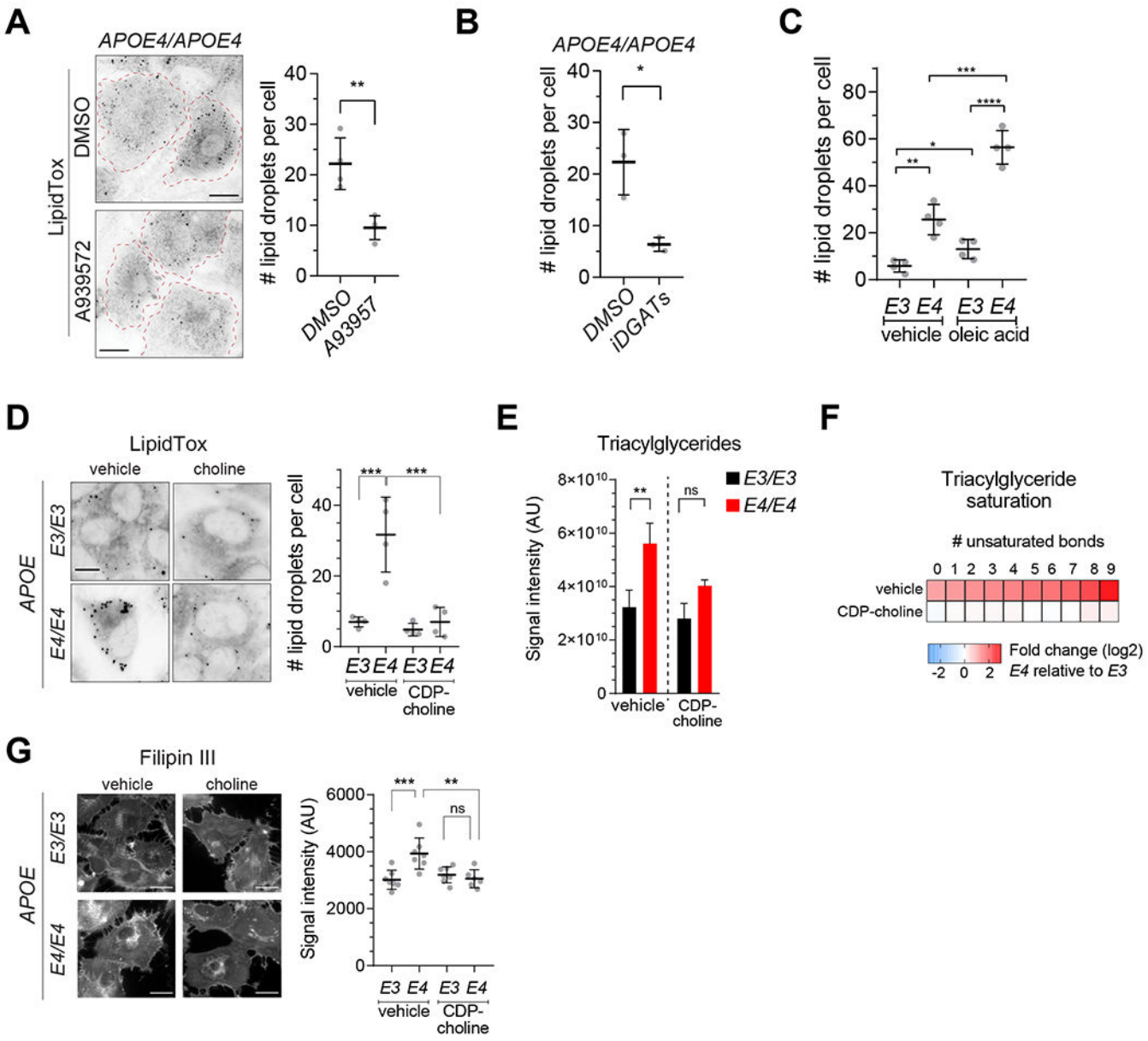

Figure 4. Modification of APOE4-induced lipid droplet accumulation in human iPSC-derived astrocytes.

(**A**) Shown are representative microscopy images of *APOE4/APOE4* iPSC-derived astrocytes treated with A939572 (inhibitor of Stearoyl-CoA desaturase-1, 100nM) or DMSO vehicle control, stained with LipidTox. Quantification of the lipid droplet number per cell is shown in the right panel. Each dot is an average of four wells with at least 20 cells measured (n=4 independent replicates). Data are represented as mean ± SD , ** $p \leq 0.01$ by Student's t-test. Scale bar, 25μm. The dashed red lines denote the boundaries of the cells. (**B**) Quantification of the lipid droplet number per cell in *APOE4/APOE4* iPSC-derived astrocytes treated with a combination of small molecule inhibitors of Diacylglycerol O-acyltransferase 1 and 2 (iDGATs, 1μM) or DMSO as vehicle control. Each dot is an average of ~50 cells analyzed. Data represent mean ± SD, * $p \leq 0.05$ by Student's t-test. (**C**)

Quantification of the number of lipid droplets in *APOE4 or APOE3* iPSC-derived astrocytes treated with oleic acid (20μM) or vehicle control (n=4 experiments, and each experiment imaged at least 20 cells). Data are represented as mean ± SD , **** $p \leq 0.0001$, ANOVA with multiple comparisons. (**D**) Representative microscopy images of *APOE4 or APOE3* iPSC-derived astrocytes stained with LipidTox after culture in media supplemented with CDP-choline (100μM) or vehicle as control. Quantification of the lipid droplet number per cell is shown in the right panel (n=4 experiments, with at least 20 cells measured per experiment). Data represent mean ± SD, *** $p \leq 0.001$ by ANOVA. (**E**) Bar graph shows intracellular triacylglycerides extracted from *APOE3* or *APOE4* iPSC-derived astrocytes grown in astrocyte media supplemented with CDP-choline (100μM) or vehicle as control. Data represent mean ± SD,with n=3 independent yeast colonies measured. ** $p \leq 0.01$ by Student's t-test. (**F**) Fold change in number of unsaturated bonds in fatty acids attached to triacylglycerides . Lipids were extracted from *APOE3* and *APOE4* iPSC-derived astrocytes grown in astrocyte media supplemented with CDP-choline (100μM) or vehicle as control. Data represent mean ± SD, n=3 experiments. (**G**) Representative microscopy images of *APOE3* and *APOE4* iPSC-derived astrocytes stained with Filipin III probe after culture in astrocyte media supplemented with CDP-choline (100μM) or vehicle as control. Quantification of Filipin III staining per cell (n=6-7 experiments, with at least 20 cells imaged) is shown in the right panel. Data represent mean ± SD, ** $p \leq 0.01$, *** $p \leq 0.001$ by ANOVA.